Master's Thesis

Investigation of the properties of high entropy alloys by ab initio calculations

Dávid Molnár

Materials Science MSc

Supervisor:
Lajos K Varga, Senior Research Fellow
Wigner Research Centre for Physics
Hungarian Academy of Sciences

Internal consultant:
Nguyen Quang Chinh
Associate Professor
Eötvös Loránd University

Eötvös Loránd University
Faculty of Science

Budapest, 2015

Abstract

This thesis will focus on single phase high entropy alloys and their ab initio calculation. It will discuss the principal points of the ab initio theory and the theory of alloys including thermodynamics and quantum mechanics. First, it will introduce the results for the metals what are included in the alloys. These results are the equilibrium volume, bulk modulus and charge density. The equilibrium volume and the bulk modulus will be compared with experimental values. The following sections will discuss alloys with different compositions. The equilibrium volume will be compared with experimental values. Since the experimental values are given at 300 K temperature, they should be extrapolated to 0 K - an extrapolation method will be introduced. There will be also a discussion about the alloy shrinking, charge density of alloys and bulk moduli of alloys. The thesis is also serves as a testing for the QNA method.

Contents

Acknowledgements

First I would like to thank my supervisor professor Lajos K. Varga for his helpfulness and endless support during the work on my thesis. I would also like to thank professor Levente Vitos for the opportunity to learn the EMTO. He and his book helped me a lot to understand the basic concepts behind his professional tool.

I would like to thank Wei Li for his continuous support for the calculations. I would like to thank Henrik Levämäki for his support and for the QNA code. I would also like to thank all of group members at the Applied Materials Physics group at KTH for their kindness and friendliness during my visits. It was a pleasure to work with them.

I would like to express my gratitude to my friends Ádám Vida and Tamás Maschefszki for their support from the beginning.

1 Introduction

1.1 Description of single phase high-entropy alloys

High-entropy alloys (*HEAs*) are containing multiple –at least four or more– elements in equimolar or near-equimolar composition. The high entropy of mixing increases the stability of the solid solutions.

Their name -HEAs- can be explained with statistical thermodynamics. The configurational entropy of a system:

$$\Delta S_{\text{conf}} = k_B \; ln\Omega, \tag{1}$$

where k is the Boltzmann's constant[1] and Ω is the multiplicity what means the number of ways in which the available energy can be mixed among the particles of the system.

The configurational entropy can be expressed by a different equation where we consider the concentration (or the mole fraction) of the elements:

$$\Delta S_{\text{conf}} = -R \sum_{i=1}^{n} c_i \; lnc_i, \tag{2}$$

where R is the gas constant[2] and c_i is the concentration of the ith element.

As an example, let's consider an equimolar alloy. The configurational entropy can be calculated as follows:

$$\Delta S_{\text{conf}} = k_B \; ln\Omega = -R \left(\frac{1}{n} ln \frac{1}{n} + \frac{1}{n} ln \frac{1}{n} + ... + \frac{1}{n} ln \frac{1}{n} \right) = -R \; ln \frac{1}{n} = R \; lnn \tag{3}$$

[1] $k_B = 1.38 \cdot 10^{23} \; J/K$
[2] $R = 8.314 \; J \cdot mol/K$

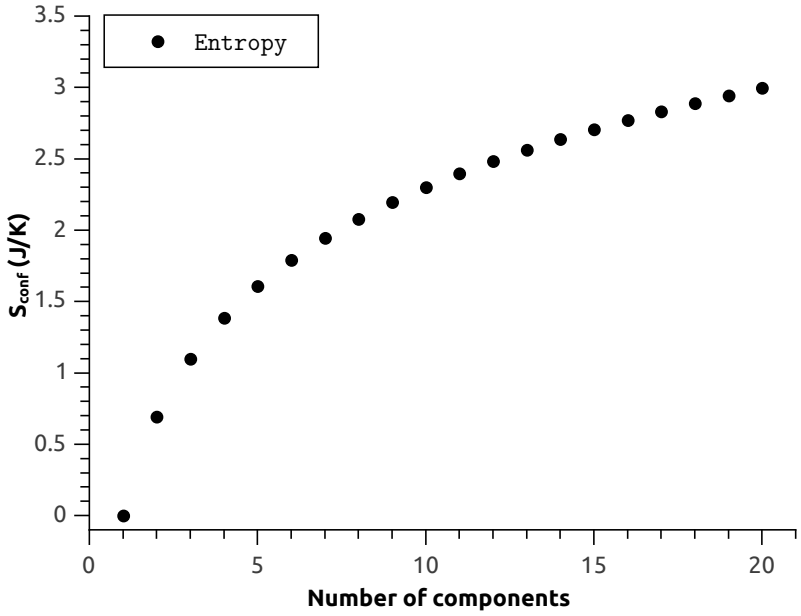

Figure 1: ΔS_{conf} plotted as the function of the number of the components in an equimolar high-entropy alloy. The ΔS_{conf} is in terms of gas constant.

On the Figure 1 one can observe how the ΔS_{conf} changes with the number of the components in an equimolar HEA. The Figure 2, shows a sketch of two equimolar systems. One of them (1;) is unmixed, and the other (2;) is mixed forming a random solid solution.

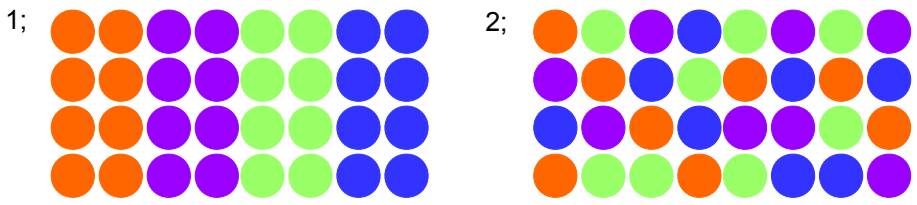

Figure 2: A 2-dimensional sketch of an equimolar unmixed (1;) and a mixed (2;) system. Different colors represent different metals. The (2;) system can be considered as a random solid solution.

Lets' look at the next equation:

$$\frac{\Delta H_f}{T_m} = \Delta S_f \sim R, \tag{4}$$

where ΔH_f is the enthalpy change per mole, T_m is the melting point, ΔS_f is the entropy change per mole and R is the gas constant. The $\Delta S_f \sim R$ means that the entropy change from solid to liquid transition is about the value of the R. $\Delta H_f \sim RT_m$. ΔH_f is the energy what needs to destroy the 1/12 of all bonds in the solid. Since the mixing entropy is quite large, it can lower the free energy of mixing, ΔG_{mix}. $\Delta G_{\text{mix}} = \Delta H_{\text{mix}} - T\Delta S_{\text{mix}}$. The decreased free energy causes the solid solution phases to have greater ability to compete with intermetallic compounds, which usually have much lower ΔS_{conf} because they are more ordered. The mixing state of constituent elements would be increased by the mixing entropy, especially at higher temperatures.

The four core effects of HEAs

High-entropy effect

This one is the most important effect. It can enhance the formation of solid solutions and makes the microstructure much simpler as expected.

There are three types of competing states:

- elemental phase,
- intermetallic compounds,
- solid solutions.

The elemental phase is the terminal solid solution based on one metal element. Intermetallic compound is a stoichiometric compound with specific superlattices. Solid solutions have all of the elements in one specific crystal structure such as BCC, FCC or HCP. From these states, the one with the lowest free energy would be in equilibrium so that would be realized.

Severe lattice distortion effect

This caused by the fact that every different atom has different neighbors. Different elements have different size and different interaction between each other what leads to distortion. This is illustrated on the Figure 3 below. One can observe that there is no unitary lattice parameter. There is only an average lattice and this can be observed by x-ray diffraction as well.

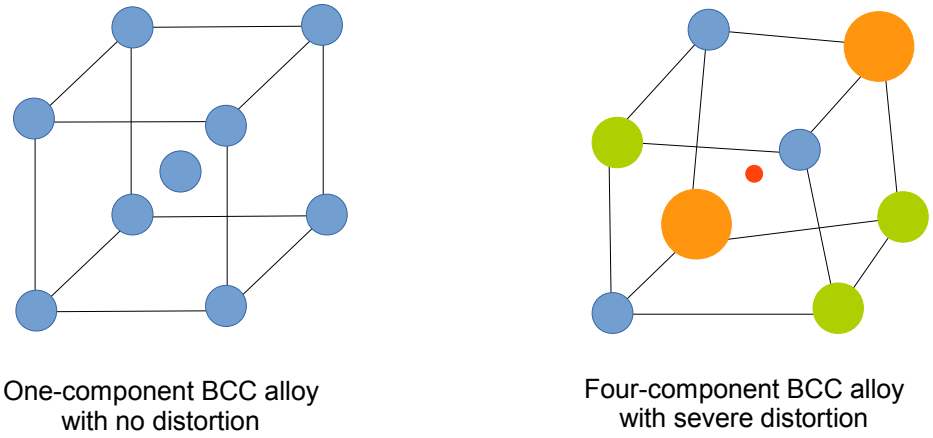

Figure 3: Schematic picture of two BCC lattices. One has only one component with no distortion, the other has five components with severe distortion

One can observe on the Figure 3 that how the lattice behaves when there are several different components in it. The bonding angles and distances are different, because of the different atomic sizes and interactions. This distortion will have a lot of effects on the properties of the alloy. For example the strength and the hardness increase. The electrical conductivity decreases because the distortion will scatter the electrons more. Phonon scattering becomes larger what decreases the thermal conductivity.

Sluggish diffusion effect

One main type of the transformations is the diffusion-controlled transformation. This kind of transformation requires cooperative diffusion of many different kind of atoms. In HEAs, the diffusion mechanism is different from the conventional alloys. It is know that in the conventional alloys, the diffusion goes by the so called „vacancy mechanism". This is when the vacancy and a nearby atom are changing their places. In HEAs, the diffusion is a bit different because there are different atoms competing to change place with the vacancy. The many different atoms will cause larger fluctuation in the lattice potential energy what can serve as barriers and traps for the diffusion of atoms. These effects are leading to the sluggish diffusion effect. This effect affects phase nucleation, distribution and growth, increased recrystallization temperature, slower grain growth, reduced particle coarsening rate. The mentioned effects can improve the properties such as strength, toughness, creep resistance, especially at high temperatures.

Coctail effect

The high-entropy alloys can be multiphase alloys as well. This means that the alloy can have several different phases depending on the composition, the processing, and other properties. The property of the whole alloy comes from these phases' overall properties. The alloy can be regarded as an atomic-scale composite, because each phase of it is a different solid solution. The properties of the composite not only come from the basic elements by the mixture rule but also from the mutual interactions between all the elements and the severe lattice distortion. These interactions and distortion give excess quantities in addition to the prediction of the mixture rule.

1.2 Review

Up to our knowledge, ab initio calculations on HEAs have been performed only in the group of Professor Levente Vitos under his guidance. A crucial point was for starting of these calculations the recognition of an average crystalline structure with an average lattice parameter necessary for the calculations. Despite the fact that the solid solution of HEAs are extremely distorted. Till now this group has published few papers[3], [4], [5].

1.3 Motivation

In order to understand and to learn the EMTO calculations based on Vitos's calculation method and code I reproduced some of earlier results of the Vitos's group in the case of $NiCoFeCrAl_x$ alloys. Getting practice in these calculations I started to calculate the electron density values. First I have calculated the electron densities for the elements and then for the alloys with known crystalline structure. Afterwards I have compared the electron densities obtainable as the average value of the elements with that calculated from the alloy. The matching of these two values bases the alloy designing using properly averaged values of the elements. This way of designing should be more efficient than the "trial and error" method.

2 Theoretical model

2.1 Ab initio theory

The final goal of this theory is to solve the Schrödinger equation for N particles. The equation for this problem is:

$$H\Psi = E\Psi, \tag{5}$$

where $\Psi = \Psi(\vec{r}_1, ..., \vec{r}_N, \vec{R}_1, ..., \vec{R}_M)$ is the N-particle wave function. $\vec{r}_i$ represents the positions of the N electrons, and $\vec{R}_j$ represents the positions of M ions. Ψ is an eigenfunction of the Hamiltonian H. The Hamiltonian is expressed as follows:

$$H = -\frac{\hbar^2}{2m_e}\sum_{i=1}^{N}\nabla_{r_i}^2 - \frac{\hbar^2}{2}\sum_{i=1}^{M}\frac{\nabla_{R_i}^2}{M_i} - q^2\sum_{i=1}^{N}\sum_{j=1}^{M}\frac{Z_j}{|\vec{r}_i - \vec{R}_j|} + \frac{q^2}{2}\sum_{i\neq j}^{N}\frac{1}{|\vec{r}_i - \vec{r}_j|} + \frac{q^2}{2}\sum_{i\neq j}^{M}\frac{Z_i Z_j}{|\vec{R}_i - \vec{R}_j|}, \tag{6}$$

where m_e is the mass of the electrons, and M_i is the mass of the ions. So, the first term is the kinetic energy of the electrons, the second is the ions. The third is the interaction between the electrons and ions. $(\vec{r}_i - \vec{R}_j)$ The fourth and the fifth parts are for the electron-electron and ion-ion interaction.

The equation becomes more simple when we apply the Born-Oppenheimer approximation. This says we can neglect the ions' kinetic energy and look at them as a static background. It is because the electrons have much less mass and they can immediately pick up the changes of the ion configuration. The H will be simplified to:

$$\left(-\frac{\hbar^2}{2m_e}\sum_{i=1}^{N}\nabla_{r_i}^2 - q^2\sum_{i=1}^{N}\sum_{j=1}^{M}\frac{Z_j}{|\vec{r}_i - \vec{R}_j|} + q^2\sum_{i\neq j}^{N}\frac{1}{|\vec{r}_i - \vec{r}_j|}\right)\Psi = (T + V_{\text{ext}} + V) = E\Psi, \tag{7}$$

where T is the kinetic energy, V_{ext} is the external potential what mentioned as static background in the Born-Oppenheimer approximation, and V is the electron-electron interaction. The most important part of the equation is the V_{ext}, because this makes the Hamiltonian unique. T and V are the same for all interacting N-electron system.

2.2 Density functional theory

The density functional theory (DFT) has introduced in the 1960s. The two founders and pioneers were Hohenberg and Kohn.[6]

The Hohenberg-Kohn theorem says that the expectation value $O = \langle\Psi|O|\Psi\rangle$ of any operator O is a unique functional of the ground state density $n(\vec{r})$, $O = O[n(\vec{r})]$. The speciality of this theorem is that we know the ground state density of a certain N-particle system, we can calculate any other system, without needing to calculate its many-body wave functions.
The ground state energy of a system can be written as a functional, since it is the expectation value of the Hamiltonian:

$$E[n] = \langle\Psi[n]|T + V_{\text{ext}} + V|\Psi[n]\rangle \tag{8}$$

The previous formalisms needs to be improved because they don't give any computational method to find the ground state density. Kohn and Sham has the solution for the problem [7].
The main idea was that to use a non-interacting system that has an external potential V_{eff} which gives the same ground state density as for the interacting system with potential V_{ext}. If the effective Hamiltonian of the non-interacting system is given by:

$$H_{\text{eff}} = T_{\text{eff}} + V_{\text{eff}}, \tag{9}$$

then its energy functional becomes:

$$E_{\text{eff}}[n] = T_{\text{eff}}[n] + \int V_{\text{eff}}(\vec{r})n(\vec{r})d\vec{r}. \tag{10}$$

Since the effective system is non-interacting, we can obtain the ground state density by first solving the Schrödinger-like single particle Kohn-Sham equations

$$(-\nabla_{r_i}^2 + V_{\text{eff}})\Psi_i = E_i\Psi_i, \tag{11}$$

where Ψ_i are the single electron orbitals. Then we perform a sum:

$$n_{\text{eff}}(\vec{r}) = \sum_{i=1}^{N} |\Psi_i(\vec{r})|^2. \tag{12}$$

The orbitals Ψ_i will correspond to the N lowest eigenvalues E_i, by virtue of the Pauli exclusion principle.

Since $n(\vec{r}) = n_{\text{eff}}(\vec{r})$ we can rewrite the equation (8) in the following way:

$$E[n] = T_{\text{eff}}[n] + \left(T[n] - T_{\text{eff}} + V[n] - \frac{1}{2} \int \int \frac{n(\vec{r})n(\vec{r}\,')}{|\vec{r} - \vec{r}\,'|} d\vec{r} d\vec{r}\,' \right) +$$
$$+ \frac{1}{2} \int \int \frac{n(\vec{r})n(\vec{r}\,')}{|\vec{r} - \vec{r}\,'|} d\vec{r} d\vec{r}' + \int V_{\text{eff}}(\vec{r}) n(\vec{r}) d\vec{r}$$
$$:= T_{\text{eff}}[n] + \frac{1}{2} \int \int \frac{n(\vec{r})n(\vec{r}')}{|\vec{r} - \vec{r}\,'|} d\vec{r} d\vec{r}' + \int V_{\text{ext}}(\vec{r}) n(\vec{r}) d\vec{r} + E_{\text{xc}}[n]. \tag{13}$$

Every information about the electron interactions, except for the Hartree term has been moved to the exchange correlation energy functional $E_{\text{xc}}[n]$. According to the Hohenberg-Kohn theorem, the ground state density should minimize the energy functional in the previous equation, (13). By taking the variation respect to $n(\vec{r})$ we get:

$$\frac{\delta E[n]}{\delta n(\vec{r})} = \frac{\delta T_{\text{eff}[n]}}{\delta n(\vec{r})} + \int \frac{n(\vec{r}\,')}{|\vec{r} - \vec{r}\,'|} + V_{\text{ext}}(\vec{r}) + V_{\text{xc}}[n(\vec{r})] = 0, \tag{14}$$

where $V_{\text{xc}}[n(\vec{r})] := \frac{\delta E_{\text{xc}}[n]}{\delta n(\vec{r})}$.

For the non-interacting system:

$$\frac{\delta T_{\text{eff}}[n]}{\delta n(\vec{r})} + V_{\text{eff}}(\vec{r}) = 0. \tag{15}$$

Inserting the equation (15) in equation (14), we get:

$$V_{\text{eff}}(\vec{r}) = V_{\text{ext}}(\vec{r}) + \int \frac{n(\vec{r}\,')}{|\vec{r} - \vec{r}\,'|} + V_{\text{xc}}(\vec{r}). \tag{16}$$

From now we have the initial guess for $n(\vec{r})$ which is used as input in the equation (16) then the V_{eff} potential is used to solve the Kohn-Sham equation (11) . The Ψ_i obtained are obtained to construct a new density from (12). Then this density is used as an input in the equation (16) to get a new potential and so on until we get a self consistent solution.

One of the most common approximation is the local density approximation (LDA), where the exchange correlation functional is assumed local:

$$E_{\text{xc}}[n] = \int \epsilon_{\text{xc}}[n] n(\vec{r}) d\vec{r}, \tag{17}$$

where ϵ_{xc} is the exchange correlation energy per electron. This can be parametrized in a many ways.

2.3 EMTO method

The exact muffin tin orbitals (EMTO) is one of the popular formalisms for solving the Kohn-Sham equations (11). This method approximates the effective potential by dividing the space into two parts. That is where its name comes from. The firs part consists of fixed radius spheres centered around the lattice sites. The potential is assumed spherically symmetric inside the spheres. The second part is between the spheres what called interstitial. The potential is constant here and it consists of planes. These conditions can be expressed as:

$$V_{\text{eff}}(\vec{r}) \approx V_{\text{mt}} := V_0 + \sum_R (V_R(r_R)) - V_0), \tag{18}$$

where $\vec{r}_R := r_R \hat{r}_R = \vec{r} - \vec{R}$ and omit the vector notation R. By definition $V_R(r_R) = V \text{for} r_R \geq s_R$. The Kohn-Sham equations are solved separately in each region. Inside the spheres, the Kohn-Sham equation (11) simplifies to a radial Schrödinger equation, and in the interstitial to a Helmholtz equation. After solving these equations using certain expanded basis functions, the problem of solving the differential equation (11) is reduced to the algebraic problem of matching the expansion coefficients.

In the EMTO method, the Kohn-Sham orbitals Ψ_i are expanded in exact muffin-tin orbitals $\overline{\Psi}^a_{RL}$, viz.

$$\Psi_i(\vec{r}) = \sum_{RL} \overline{\Psi}^a_{RL}(E_i, \vec{r}_R) v^a_{RL,i}, \tag{19}$$

where $v^a_{RL,i}$ are the expansion coefficients, chosen such that the equation (19) solves the Kohn-Sham equation in all space. We use the formalism that $L := (l, m)$, where l is the orbital-, and m is the magnetic quantum number respectively. For the interstitial region we use screened potential spherical waves $\overline{\Psi}^a_{RL}$ as basis functions, which solves the Helmholtz equation

$$(\nabla^2 + \kappa^2)\overline{\Psi}^a_{RL}(\kappa^2, \vec{r}_R) = 0, \tag{20}$$

where $\kappa^2 := E - V_0$, and E is the energy. The boundary conditions for this equation are given in combination with non-overlapping spheres with radius a_R centered around R. Inside the spheres the basis functions are chosen to be partial waves, which are products of the solution to the radial Schrödinger equation,

$$\frac{\partial^2(r_R \phi_{Rl}(E, r_R))}{\partial r^2} = \left(\frac{l(l+1)}{r_R^2} + V_R(r_R) - E \right) r_R \phi_{RL}(E, r_R), \tag{21}$$

and real spherical harmonics, viz.

$$\phi^a_{RL}(E, \vec{r}_R) \sim \phi_{RL}(E, r_R) Y_L(\hat{r}_R). \tag{22}$$

They are defined for general complex energies and for $r_R \geq s_R$. The matching condition should now be set up between $\phi^a_{RL}(E, \vec{r}_R)$ and $\Psi^a_{RL}(\kappa^2, \vec{r}_R)$ at a_R. However, since we want the possibility of overlapping potential spheres, usually $s_R > a_R$. Hence a free electron solution $\Phi^a_{RL}(R, \vec{r}_R)$ is introduced, which joins continuously and differentiable to the partial waves at s_R and continuously to the screened spherical wave at a_R. Matching of all coefficients will lead to the kink cancellation equation,

$$\sum_{RL}(S^a_{RLR'L'}(\kappa_i^2) - \delta_{RR'}\delta_{LL'}D^a_{RL}(E_i))v^a_{RL,i} = 0, \tag{23}$$

where D^a_{RL} denotes to the EMTO logarithmic derivative function[8],[9], and $S^a_{RLR'L'}$ is the slope matrix[10]. This defines the kink matrix for a general complex energy z, viz.

$$K^a_{RLR'L'}(z) := \delta_{RR'}\delta_{LL'}D^a_{RL}(z) - S^a_{RLR'L'}(z). \tag{24}$$

A solution of the equation (23) will give the single electron eigenvalues E_i and wave functions Ψ_i. The EMTO method solves the equation (23) by the Green's function method, which uses the path operator $g^a_{R'L'RL}$, defined as the inverse of the kink matrix (24),

$$\sum_{R''L''} K^a_{R'L'}(z)g^a_{R''L''RL}(z) := \delta_{RR'}\delta_{LL'}. \tag{25}$$

The eigenvalues will be the poles of $g^a_{R'L'RL}(z)$. This is a green's function, since it is the inverse of the operator $(z - H_{\text{eff}})$, hence the name *Green's function method*. If we have translational symmetry, the sum over site index in equation (23) and (25) is over the atoms in the primitive cells. The kink matrix, path operator and slope matrix will then depend on the Bloch k-vector in the first Brillouin zone.

Since the energy derivative of the kink matrix, $\dot{K}^a_{RLR'L'}(z)$, gives the overlap matrix for the EMTO basis set, the matrix elements of the properly normalized Green's function become

$$G_{RLR'L'}(z) = \sum_{R''L''} g^a_{RLR''L''}(z)\dot{K}^a_{R''L''R'L'}(z) - \delta_{RR'}\delta_{LL'}I^a_{RL}(z), \tag{26}$$

where $I^a_{RL}(z)$ accounts for the non-physical poles of $\dot{K}^a_{RLR'L'}(z)$. The total number of states at the Fermi level E_F is obtained by using the Cauchy residue theorem, viz.

$$N(E_F) = \frac{1}{2\pi i}\sum_{RLR'L'}\oint G_{RLR'L'}(z)dz, \tag{27}$$

where the energy integral is carried out along a complex contour that cuts the real axis below the bottom of the valence band at the E_F. The charge density is computed on the same complex contour. The formalism can be generalized to include spin.

2.3.1 Coherent Potential Approximation

The coherent potential approximation was introduced by Soven[11] for the electronic structure problems and by Taylor[12] for phonons in random alloys. Later, Györffy[13] formulated the CPA in the framework of the multiple scattering theory using the Green function technique. The CPA is based on the assumption that the alloy may be replaced by an ordered effective medium, the parameters of which are determined self-consistently. The impurity problem is treated within the single site approximation. This means that one single impurity is placed in an effective-medium and no information is provided about the individual potential and charge density beyond the sphere or polyhedron around this impurity. The principal idea of the CPA within the muffin-tin formalism illustrated below. We consider a substitutionary $A_aB_bC_c...$, where the atoms $A, B, C, ...$ are randomly distributed in the underlying crystal structure. Here $a, b, c, ...$ stand for the atomic fractions of the $A, B, C, ...$ atoms, respectively. This system is characterized by the Green function g and the alloy potential P_{alloy}. The latter, due to the environment, shows small variations type of the atoms. There are two main approximations within the CPA. First, it is assumed that the local potentials around a certain type of atom from the alloy are the same i.e. the effect of local environments is neglected. These local potentials are described by the potential functions $P_A, P_B, P_C, ...$ Second, the system is replaced by a monoatomic setup described by the site independent coherent potential $\tilde{P}$. In terms of Green functions, one approximates the real Green function g by a coherent Green function $\tilde{g}$. For each alloy component $i = A, B, C, ...$ a single-site Green function g_i is introduced.

The main steps to construct the CPA effective medium are as follows. First, the coherent Green function is calculated from the coherent potential using an electronic structure method. Within the Korringa−Kohn−Rostoker (KKR) or Linear Muffin-Tin Orbital (LMTO) methods, we have

$$\tilde{g} = \left[S - \tilde{P}\right]^{-1} \tag{28}$$

where S denotes the KKR or LMTO structure constant matrix corresponding to the underlying lattice. Next, the Green functions of the alloy components, g_i, are determined by substituting the coherent potential of the CPA medium by the real atomic potentials P_i. Mathematically, this condition is expressed via the real-space Dyson equation

$$g_i = \tilde{g} + \tilde{g}(P_i - \tilde{P})g_i \ , \ i = A, B, C... \tag{29}$$

Finally, the average of the individual Green functions should reproduce the single-site part of the coherent Green function, i.e.

$$\tilde{g} = ag_A + bg_B + cg_C + ... \tag{30}$$

Equations (29), (30) are solved iteratively, and the output $\tilde{g}$ and g_is are used to determine the electronic structure, charge density and total energy of the random alloy.

2.4 Exchange-correlation approximations

I will present a few expressions for the exchange-correlation functionals used in the density functional calculations.

2.4.1 LDA - Local Density Approximation

As I mentioned before there is a very common approximation, the Local Density Approximation (LDA). The exchange-correlation energy can be written as:

$$E_{xc}[n] = E_x[n] + E_c[n] = \int n(\vec{r})\epsilon_x([n];\vec{r})d\vec{r} + \int n(\vec{r})\epsilon_c([n];\vec{r})d\vec{r}, \tag{31}$$

where $\epsilon_x([n];\vec{r})$ and $\epsilon_c([n];\vec{r})$ represents the exchange and the correlation energies per electron, respectively.

In spin polarized case one can write the following equation for the exchange energy:

$$E_x[n_\uparrow, n_\downarrow] = (E_x[2n_\uparrow] + E_x[2n_\downarrow])/2, \tag{32}$$

where $n_\uparrow$ and $n_\downarrow$ are the spin-up and spin-down electron densities, respectively.

For a uniform non-polarized electron gas, the exchange energy per electron is:

$$\epsilon_x(n) = -\frac{3}{2}\left(\frac{3}{\pi}\right)^{1/3} n^{1/3}. \tag{33}$$

The exchange potential is the density derivative of $n \cdot \epsilon_x(n)$:

$$\mu_x(n) = -2\left(\frac{3}{\pi}\right)^{1/3} n^{1/3}. \tag{34}$$

2.4.2 GGA - Generalized Gradient Approximation

In the Generalized Gradient Approximation[14], the exchange energy per electron is:

$$\epsilon_x(n, s) = \epsilon_x(n)F_x(s), \tag{35}$$

where

$$s = \frac{|\nabla n|}{2k_F n}, \tag{36}$$

what is the dimensionless or reduced density gradient, $k_F = (3\pi^2 n)^{1/3}$, and

$$F_x(s) = 1 + \kappa - \frac{\kappa}{1 + \mu s^2/\kappa}, \tag{37}$$

with $\kappa = 0.804$ and $\mu = 0.21951$.

The GGA correlation energy per electron is given as:

$$\epsilon_c(r_s, \eta) = \epsilon_c(r_s, \eta) + H(r_s, \eta, t), \tag{38}$$

where

$$t = \frac{|\nabla n|}{2k_s g(\eta) n}, \tag{39}$$

$k_s = (4k_F/\pi)^{1/2}$,

$$g(\eta) = \frac{(1+\eta)^{2/3} + (1-\eta)^{2/3}}{2}, \tag{40}$$

and $\eta = \frac{n_\uparrow - n_\downarrow}{n_\uparrow + n_\downarrow}$. The $H(r_s, \eta, t)$ is given by:

$$H(r_s, \eta, t) = \gamma g(\eta)^3 ln \left\{ 1 + \frac{\beta}{\gamma} t^2 \left[\frac{1 + \xi t^2}{1 + \xi t^2 + \xi^2 t^4} \right] \right\}, \tag{41}$$

where

$$\xi = \frac{\beta}{\gamma} \frac{1}{exp[-\epsilon_c^{LDA}(n)/2\gamma g(\eta)^3] - 1}, \tag{42}$$

$\gamma = 0.031091$ and $\beta = 0.066725$.

2.4.3 QNA - Quasis non-local gradient level exchange-correlation approximation

The quasi-non-uniform gradient-level exchange-correlation approximation[15], [16] is a really new approach of exchange correlation, it was published first in 2012.

The aim of this exchange correlation is to give more accurate results. It divides the selected system into subsystems. Each subsystem functional has its own optimal parameters (μ, β) determined by the element-specific valence-core overlap region. The overall functional can be written as a superposition of the subsystem functionals:

$$E_{xc}^{QNA}[n] = \sum_q \int_{\Omega_q} \epsilon_x^{LDA}(n) F_{xc}^{opt_q}(r_s, s) d^3 r, \tag{43}$$

where $F_{xc}^{opt_q}$ is the PBE/PBEsol enhancement function based on μ, β_{opt_q} optimized for the alloy component q. The integration domain is within Ω_q around each atomic site q.

The optimal values for μ and β can be chose by finding such parameters what are minimizing

$$\frac{|V_0 - V_{\text{expt}}|}{V_{\text{expt}}} + \frac{|B_0 - B_{\text{expt}}|}{B_{\text{expt}}}, \tag{44}$$

where V_0 is the equilibrium volume and B_0 is the equilibrium bulk modulus.

2.5 Calculation of the electron density n

Within the Spherical Cell Approximation (SCA)[10], supposing that the electron density in the interstitial region equals to the electron density at the surface at the Wigner-Seitz sphere the electron density can be calculated from the output of the ab initio calculation which gives:

$$Q = 4\pi w^2 n(w). \tag{45}$$

Where from the $n(w)$ can be calculated using the Wigner-Seitz radius w. Calculation of this $n(w)$ is straightforward both for the constituent elements and for the HEA alloys.
In the section of the results (Chapter 3.3) of this thesis we are going to compare the electron density value obtained for the alloys with the weighted average value of the elements.

2.6 Ground-state properties

The equilibrium Wigner-Seitz radius have been calculated for every metal what are used in this thesis. It is obtained by calculating the energies for several radii around the experimental value then I fitted the equation of state (EOS)(46) to the points . The result of a fitting is shown below on the Figure 4.

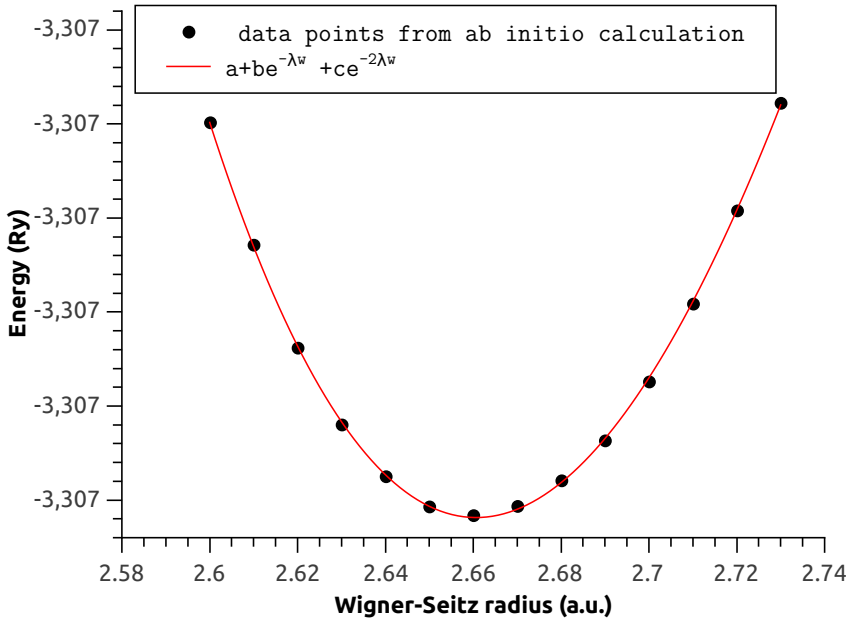

Figure 4: An example of an equation of state fitting for copper. In practice, I use fewer points. I fitted the $E(w) = a + be^{-\lambda w} + ce^{-2\lambda w}$ equation, where the w is the Wigner-Seitz radius in Bohr units. For this fitting, I got $w = 2.661$ a.u. what has good agreement with the experimental data.

I worked with a Morse-type equation of state:

$$E(w) = a + be^{-\lambda w} + ce^{-2\lambda w} \tag{46}$$

where $E(w)$ is the total energy in terms of the Wigner-Seitz radius w, and a, b, c, and λ are independent Morse parameters.

[2] $1\ a.u. = 0,529177211$ Å

By $x = e^{-\lambda w}$:

$$E(w) = a + bx + cx^2 \tag{47}$$

The pressure can be calculated from the total energy:

$$P = -\frac{\partial E}{\partial V}, \tag{48}$$

where $V = \frac{4}{3}\pi w^3$ is the volume of the Wigner-Seitz cell.

$$P = \frac{x\lambda^3}{4\pi(lnx^2)}(b + 2cx) \tag{49}$$

Since the pressure vanishes at $r = w$, where $(b + 2cx = 0)$ and $x = x_0$,

$$x_0 = -\frac{b}{2c}, \tag{50}$$

and

$$w = -\frac{lnx_0}{\lambda}. \tag{51}$$

Here, w is the equilibrium Wigner-Seitz radius.

Bulk modulus (B) is defined as

$$B = -V\,\frac{\partial P}{\partial V}, \tag{52}$$

then becomes

$$B = -\frac{x\lambda^3}{12\pi lnx}\left[(b + 4cx) - \frac{2}{lnx}(b + 2cx)\right]. \tag{53}$$

Since $(b + 2cx) = 0$ at w, where $x = x_0$,

$$B(w) = -\frac{cx_0^2\lambda^3}{6\pi lnx_0}. \tag{54}$$

One should consider that these values can slightly differ even at zero temperature because of the zero-point energy.

2.7 Lattice parameters

In this section I am going to introduce the two basic types of cubic crystal structures what are occuring in high entropy alloys. Some elements such as manganese have different type of crystal structure but in that case I will discuss it in the related section. For each calculation I got the results as the Wigner-Seitz radius of the element. They will be converted to lattice parameters because it is easier to understand and most of the papers are using this kind of unit to compare their results.

Wigner-Seitz radius

The Wigner-Seitz radius (w) is the radius of a sphere whose volume is equal to the average volume per atom in solid. So this radius can be imagined as the radius of the small hard spheres what are building up the whole solid.

One can get w by this equation:

$$w = \left(\frac{3M}{4\pi\rho N_A} \right)^{1/3}, \tag{55}$$

where M is the molar mass, ρ is the density of the system and N_A is the Avogadro number.

The Wigner-Seitz volume is calculated using w by the next equation:

$$V_{WS} = \frac{4}{3}\pi w^3 \tag{56}$$

Face centered cubic structure

This is a cubic structure so I can approximate its volume by calculating the volume of a cube.

$$N\frac{4\pi}{3}w^3 = V \tag{57}$$

N is the number of the atoms in the unit cell ($= 4$), w is the Wigner-Seitz radius, V is the volume of the unit cell. Since this is a cube, the edges are equally long so the $V = a^3$ equation is valid. The a is the lattice constant.
Using the hard spheres model, the lattice parameter can be expressed in terms of the Wigner-Seitz radius:

$$\sqrt[3]{\frac{16\pi}{3}w^3} = a \tag{58}$$

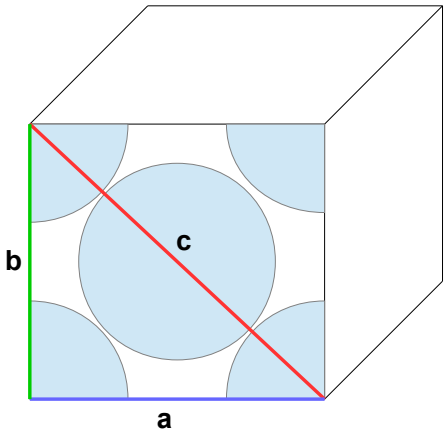

Figure 5: Sketch of the face centered cubic cell. One can see the atomic arrangement on the face of the the unit cell.

By the Figure 5 one can easily understand the correlation between the atomic radius and the lattice constant. Since a and b are the edges of the unit cube and c is the face diagonal one can easily use the Pythagorean theorem:

$$a^2 + b^2 = c^2, \tag{59}$$

where a, b and c are the corresponding lines on the Figure 5. One can see that the c can be expressed as $4r$ since there are two half and a whole atom on the face of the cube and $a = b$. So, the Pythagorean equation will be:

$$2a^2 = (4r)^2 \rightarrow 2a^2 = 16r^2 \rightarrow r = \frac{\sqrt{2}}{4}a \tag{60}$$

Body centered cubic structure

The volume of the unit cell can calculated by the next equation:

$$N\frac{4\pi}{3}w^3 = V \tag{61}$$

N is the number of the atoms in the unit cell ($= 2$), w is the Wigner-Seitz radius, V is the volume of the unit cell. Since this is a cube, the edges are equally long so the $V = a^3$ equation is true. The a is the lattice constant.

The lattice parameter can be expressed in terms of Wigner-Seitz radius:

$$\sqrt[3]{\frac{8\pi}{3}w^3} = a \tag{62}$$

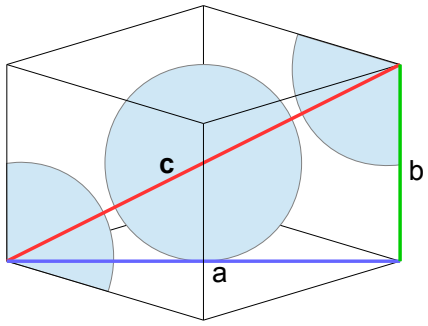

Figure 6: Sketch of the body centered cubic cell. One can see the atomic arrangement in the unit cell.

By observing Figure 6, one can easily calculate and understand the results by simple geometry. First, let's calculate a. Since all the edges are equal, we get the next equation:

$$b^2 + b^2 = a^2 \rightarrow \sqrt{2}b = a \tag{63}$$

We have a and b, so it will be easy to find c:

$$a^2 + b^2 = c^2 \rightarrow (\sqrt{2}b)^2 + b^2 = c^2 \rightarrow \sqrt{3}b = c, \tag{64}$$

where b is the lattice constant and $c = 4r$, so:

$$r = \frac{\sqrt{3}}{4}a \tag{65}$$

Extrapolation to 0 K and ZPAE

As the literature mostly have room temperature values for the lattice parameters, I had to apply an approximated extrapolation to zero Kelvin.
The thermal expansion can be expressed by the next formula:

$$\frac{\Delta V^{(1)}}{V} = \int_0^{T_{\mathrm{rt}}} \alpha_V(T) dT, \tag{66}$$

where $\Delta V^{(1)}$ is the volume change, V is the total volume, $\alpha_V(T)$ is the temperature dependent volume-expansion coefficient. It is zero at 0 K and $\alpha_{V,rt}$ at room temperature.

Since $\Delta V^{(1)}$ constitutes only a small correction with respect to the total volume V, the equation (66) can be approximated as:

$$\frac{\Delta V^{(1)}}{V} \approx \int_0^{T_{\mathrm{rt}}} \alpha_{V,rt} \frac{T}{T_{rt}} dT = \frac{\alpha_{V,rt} T_{rt}}{2}. \tag{67}$$

The original approach is calculated by volumes but since these are cubic structures, it is enough to use the edges of the cubic cell what are the lattice parameters of each elements or alloys. So I am going to introduce an average thermal expansion coefficient $\alpha^* = \frac{\alpha_{V,rt}}{6}$. The equation for a_0 will be written as:

$$a_0 = \frac{a_{\mathrm{expt}}}{1 + \alpha^* T_{\mathrm{rt}}}, \tag{68}$$

where a_0 stands for the 0 K lattice parameter in Ångström, a_{expt} is the experimental lattice parameter in Ångström, α^* is the thermal expansion coefficient in $10^{-6} K^{-1}$ unit, and T_{rt} is the room temperature in Kelvin.

The thermal expansion can be corrected further by applying the correction for zero-point anharmonic expression:

$$a_{0+\mathrm{ZPAE}} = \frac{a_{\mathrm{expt}}}{1 + \alpha^* T_{\mathrm{rt}}} - a_{\mathrm{ZPAE}}, \tag{69}$$

The order of magnitude of this correction is around $0,005$ Å for each elements. The exact values are included in the Table 1. These equations can only be used for single element.
For alloys, I used the weighted average of the values.

$$\overline{\alpha^*} = \sum_{i=1}^{n} c_i \alpha_i^*, \tag{70}$$

where $\overline{\alpha^*}$ is the weighted average of the thermal expansion coefficients, c_i is the concentration of ith element, and α_i^* is the thermal expansion coefficient of the ith element.

I calculated the weighted average of the ZPAE the same way:

$$\overline{\text{ZPAE}} = \sum_{i=1}^{n} c_i \text{ZPAE}_i \tag{71}$$

$\overline{\text{ZPAE}}$ is the weighted average of the zero-point anharmonic coeffitient, c_i is the concentration of the *ith* element, and ZPAE is the zero-point anharmonic coefficient of *ith* element.

The Table 1 below has the $\alpha_{V,rt}$, α^*, and ZPAE values for those elements what I used for the calculations for the alloys.

Element	$\alpha_{V,rt}(10^{-6}K^{-1})$	$\alpha^*(10^{-6}K^{-1})$	ZPAE (Å)
Al	69,3	34,65	0,012
Cr	14,7	7,35	0,008
Fe	71,4	35,7	0,008
Ni	40,2	20,1	0,008
Cu	49,5	24,75	0,007
Co	41,1	20,55	0,005
V	25,2	12,6	0,004
Nb	21,9	10,95	0,002
Mn	124,8	62,4	0,008
Pd	35,4	17,7	0,004
Ta	18,9	9,45	0,002
W	13,5	6,75	0,002

Table 1: Thermal expansion coefficients [18] [19] and ZPAE values [20] [21] for the extrapolation

VED (n) and VEC

These two definitions should be discussed. The VEC is the valence electron concentration what is simply is the number of valence electrons for each element, respectively. For example the VEC of the aluminum is 3. This is a really simple but powerful number to describe the system. It has been used to make a difference between crystal structures [22], [23], [24]. They describe the BCC-FCC transition differently by the change in the value of the VEC. The same rules will be applied in this thesis.

The VED is the valence electron density. This can be determined relative to the Wigner-Seitz volume (56):

$$\text{VED} = n(w) = \frac{\text{z}}{V_{WS}}, \tag{72}$$

Where VED $= n(w)$ is the charge density, z is the valence and V_{WS} is the Wigner-Seitz volume.

The value of the VED is subject of debate. The results can be very different because of the different calculation of V_{WS} and z. Some people are suggesting quantities to use such as metallic valence or bonding valence. In this thesis I will investigate some of these values and that how they line up against the results of the ab initio calculation.

Charge density for alloys

Since I calculated this value for alloys as well, I needed to calculate the weighted average of this value. I calculated the charge density by getting $n(w)$ of each elements, then summarized them weighted with their concentration in the alloy.

$$n(w)_{\text{eff}} = \sum_{i}^{n} c_i n(w)_i \tag{73}$$

$n(w)_{\text{eff}}$ is the effective charge density of the alloy, c_i is the concentration of the ith element, and $n(w)_i$ is the charge density of the ith element.

3 Results

In this section I will summarize the results for high-entropy alloys and their elements as well. I will try to find some correlations between them. The most important goal was to be able to run the ab initio calculations, extract the results and understand them. The main aspect of the thesis is the lattice parameters but I will try to explain something about the charge density or better known as valence.

3.1 Results for elements

3.1.1 Lattice parameters

The lattice parameters have been calculated for the elements used in high entropy alloys in this thesis. I compared the results of the ab initio calculation with different results in order to get a picture of the accuracy of my calculations.

Element	$a_{\text{tabulated}}$ (Å)	$a_{\text{ab initio}}$ (Å)	a_{expt} (Å)
Al	4,048	4,019	4,020
V	3,028	3,023	3,024
Cr	2,891	2,800	2,877
Mn	2,905	2,925	2,910
Fe	2,866	2,850	2,853
Co[3]	2,503	2,485	2,498
Ni	3,524	3,508	3,508
Cu	3,616	3,602	3,595
Nb	3,300	3,288	3,294
Mo	3,141	3,136	3,141
Pd	3,888	3,883	3,875
Ta	3,302	3,282	3,299
W	3,164	3,168	3,160

Table 2: Calculated lattice constants compared with experimental data

The reader can see three different columns for the lattice parameters in Table 2. $a_{\text{tabulated}}$ is calculated from the molar mass and density from the periodic table [18], $a_{\text{ab initio}}$ is calculated by ab initio and a_{expt} are the experimental datas[18], respectively. The experimental data is extrapolated to zero Kelvin using the thermal expansion coefficient and zero-point anharmonic expansion. As one can see, these results have only slight difference.

[3]The results for cobalt from a calculation using PBE (GGA) instead of QNA. It is because it has HCP structure and QNA is not capable of handling HCP structures yet.

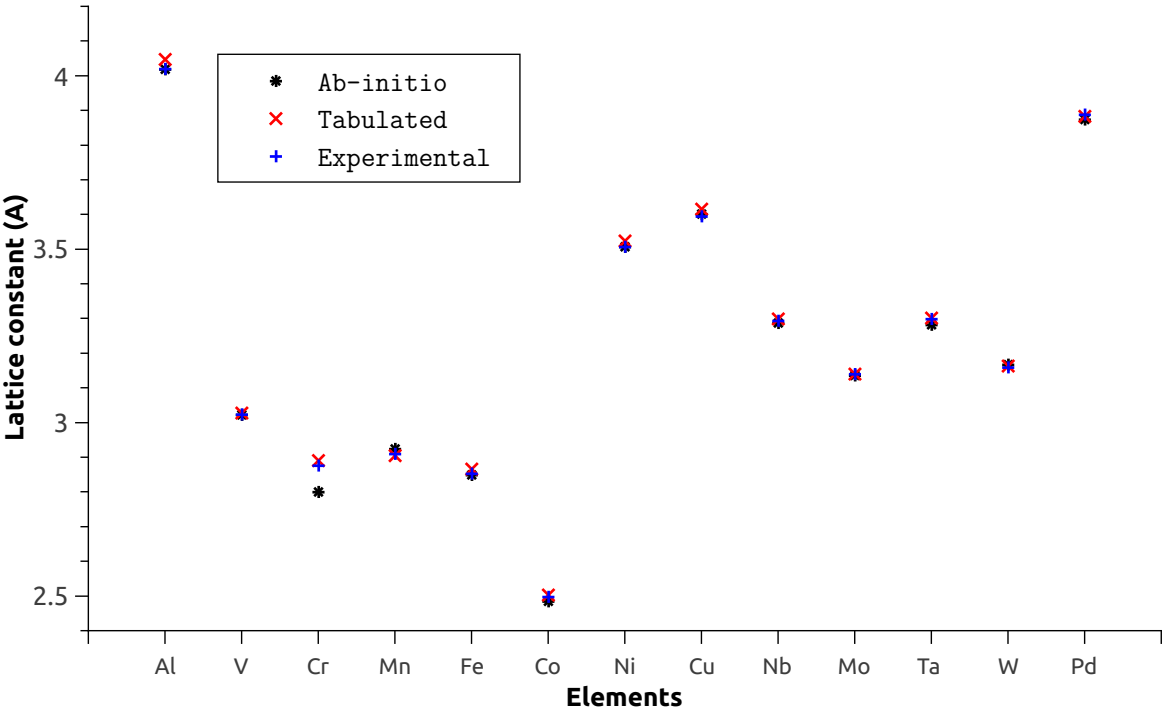

Figure 7: Comparison for lattice constants of different elements and calculation methods

3.1.2 Charge density

After I obtained the equilibrium lattice parameters for the required metals I calculated the charge density for them. As it is stated in the Section 2.5 one can obtain Q as a result of the ab initio calculation. Rearranging the equation (45) for $n(w)$ and substituting w into the formula, the value of the charge density can be obtained:

$$n(w) = \frac{Q}{4\pi w^2}. \tag{74}$$

The valence electron density can be expressed from $n(w)$ by multiplying it by the Wigner-Seitz volume (V_{WS}):

$$n(w) = \frac{z}{V_{WS}} \rightarrow z = n(w)\ V_{WS}, \tag{75}$$

where $n(w)$ is the electron density in $\frac{e^-}{\text{Å}^3}$, z is the valence as the number of electrons and V_{WS} is the atomic volume in Å^3 units.

For the $n_{\text{ab initio}}$ results, V_{WS} came from the fitting of the equation of state (46), for n_{UMEG}[4], V_{WS} is calculated from the atomic radii used from the paper [25], for $n_{\text{tabulated}}$, V_{WS} is calculated from the density and the molar mass of the element (55) and z is referred as the nominal valence used in [25].

Element	$n_{\text{ab initio}}$	$z_{\text{ab initio}}$	n_{UMEG}	z_{UMEG}	$n_{\text{tabulated}}$	$n_{\text{tabulated}}$
Al	0,182	2,948	0,167	2,76	0,181	3
V	0,242	3,347	0,251	3,45	0,360	5
Cr	0,303	3,523	0,295	3,53	0,497	6
Mn	0,317	3,462	0,279	3,41	0,245	3
Fe	0,274	3,174	0,285	3,33	0,340	4
Co	0,305	3,147	0,268	3,03	0,364	4
Ni	0,267	2,880	0,256	2,83	0,366	4
Cu	0,225	2,630	0,220	2,57	0,254	3
Nb	0,232	4,120	0,233	4,14	0,278	5
Mo	0,289	4,452	0,283	4,42	0,388	6
Pd	0,231	3,384	0,215	3,15	0,272	4
Ta	0,254	4,495	0,254	4,51	0,278	5
W	0,311	4,937	0,489	7,79	0,379	6

Table 3: Comparison of different $n\left(\frac{e^-}{\text{Å}^3}\right)$ and z values.

[4]UMEG: Uniform Metallic Electron Gas

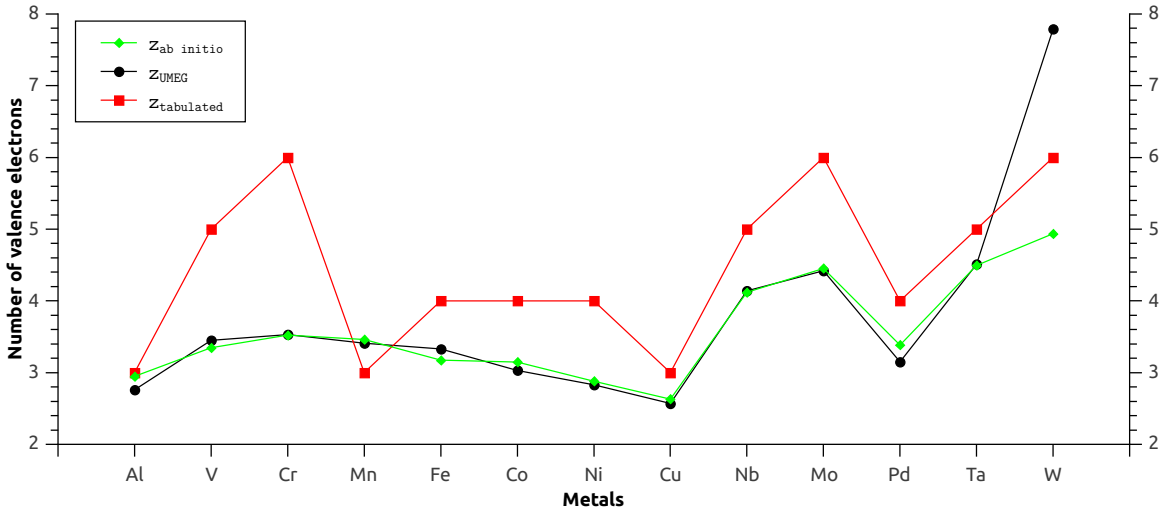

Figure 8: Comparison for valences (z) for different datas

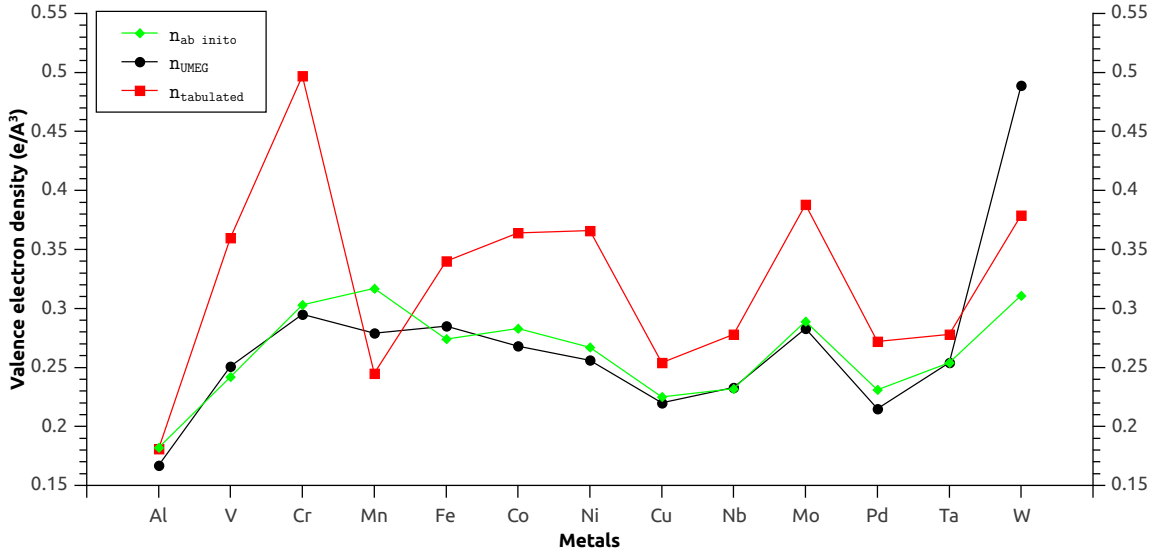

Figure 9: Comparison for valence electron densities (n) for different datas

For both Figure 8 and Figure 9 there are good agreements between the ab initio and UMEG results. This suggests that the ab initio calculation gives the bonding valence as the result, defined by H,B. Shore and J.H. Rose [26].

3.1.3 Bulk Modulus

As it is mentioned in the earlier section (Section 2.6), one can get the bulk modulus from the results of the ab initio calculation by fitting the equation of state curve and substituting the parameters to the equation for the equilibrium bulk modulus (54). I have collected these results for the metals used in this thesis into the Table 7.

Since I investigated some literature I found other way to get the bulk modulus from experimental data [27]. The one I found very interesting is based on the next equation:

$$n_{WS} = 6,748 \cdot 10^{-2} \sqrt{\frac{B}{V_m}}, \tag{76}$$

where n_{WS} is the valence electron density (75), B is the bulk modulus in GPa and V_m is the molar volume in cm^3/mol. The original equation is used for calculate the charge density but since I have the n_{WS} and V values, I am going to calculate the B.

Element	V_m (cm^3/mol)	n_{WS}	B (GPa)
Al	9,771	2,693	70,857
V	8,314	3,592	107,281
Cr	7,012	4,484	140,957
Mn	6,583	4,694	145,034
Fe	6,967	4,066	115,185
Co	6,222	4,513	126,743
Ni	6,499	3,954	101,612
Cu	7,037	3,336	78,300
Nb	10,699	3,437	126,376
Mo	9,287	4,278	169,950
Pd	8,816	3,426	103,471
Ta	10,648	3,768	151,149
W	9,569	4,604	202,820

Table 4: Calculated B where both V_m and n_{WS} obtained from ab initio calculation

Element	$V\ (cm^3/mol)$	n_{WS}	$B\ (GPa)$
Al	9,987	2,681	71,767
V	8,361	5,337	238,127
Cr	7,268	7,367	394,448
Mn	7,376	3,630	97,171
Fe	7,086	5,038	179,821
Co	6,615	5,396	192,632
Ni	6,586	5,420	193,473
Cu	7,116	3,762	100,721
Nb	10,824	4,122	183,942
Mo	9,321	5,745	307,593
Pd	8,841	4,038	144,128
Ta	10,844	4,115	183,603
W	9,540	5,613	300,540

Table 5: Calculated B where V_m calculated from M and ρ by using equation (55) and n_{WS} obtained from [26] as *nominal valence*

Element	$V\ (cm^3/mol)$	n_{WS}	$B\ (GPa)$
Al	9,924	2,477	60,910
V	8,279	3,712	114,084
Cr	7,182	4,378	137,673
Mn	7,344	4,136	125,638
Fe	7,022	4,224	125,299
Co	6,787	3,977	107,330
Ni	6,634	3,800	95,798
Cu	7,022	3,260	74,632
Nb	10,691	3,450	127,216
Mo	9,385	4,195	165,176
Pd	8,820	3,181	89,265
Ta	10,691	3,758	150,971
W	9,579	7,244	502,705

Table 6: Calculated B where V_m calculated from the atomic radius[26] using (56) and n_{WS} obtained from [26] as *bonding valence*

	B (GPa)				
Element	Experimental	ab initio EOS	Table 6.	Table 7.	Table 8.
Al	76	81,36	70,86	71,77	60,91
V	160	166,33	107,28	238,13	114,08
Cr	160	241,56	140,96	394,45	137,67
Mn	120	247,15	145,03	97,17	125,64
Fe	170	162,05	115,18	179,82	125,30
Co	180	256,75	126,74	192,63	107,33
Ni	180	203,61	101,61	193,47	95,80
Cu	140	161,76	78,30	100,72	74,63
Nb	170	155,90	126,38	183,94	127,22
Mo	230	229,10	169,95	307,59	165,18
Pd	180	197,07	103,47	144,13	89,26
Ta	200	189,01	151,15	183,60	150,97
W	310	310,42	202,82	300,54	502,71
Mean absolute deviation		30,30	52,79	43,70	61,23

Table 7: Comparison for different bulk moduli

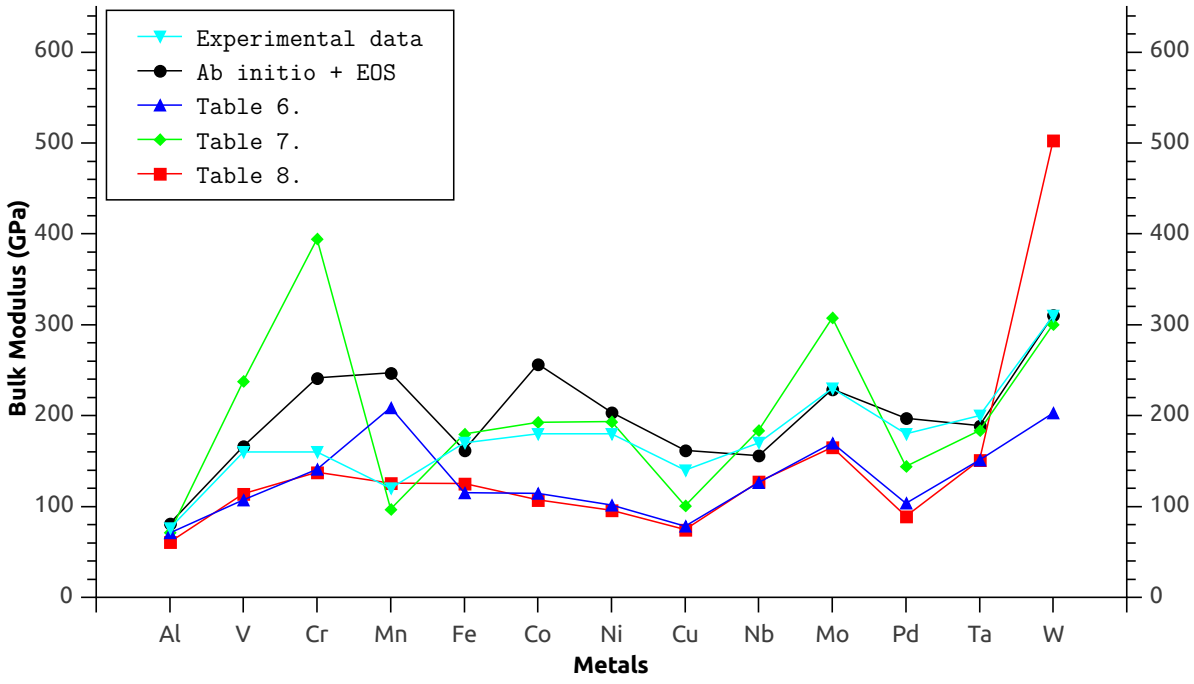

Figure 10: Comparison for different Bulk moduli

I compared five different bulk moduli. The experimental data is from [28], [29], [30]. The *ab initio + EOS* is calculated using the equation of state fitting (8). The Table 6-7-8 are described in their captions.

The results of Table 6 and Table 8 are following each other very closely but this is what I expected because n_{UMEG} and $n_{\mathrm{ab\ initio}}$ values are either following each other as I shown it in Figure 9. They are somewhat close to the experimental data too but at least they are following the same trend. The best results obtained by the equation of state fitting. That method has the lowest mean absolute deviation. The second best is the results for Table 7. There are some huge differences such as for chromium or molybdenum but most of the elements are close to the experimental value.

3.2 Results for alloys

In this section I am going to introduce my results for different single phase high entropy alloys. The main topic will be the determination of the equilibrium Wigner-Seitz radius, the bulk modulus and the VED. I can only compare the results of Wigner-Seitz radii with experimental ones. I calculated each elements lattice constants from their Wigner-Seitz radius by (62) and (58), respectively. The experimental data [4] were extrapolated to zero Kelvin temperature what is detailed in the Section 2.7.

Since I do not have any data for VED and bulk modulus to compare to, I will investigate that how the different approaches are differ from each other. These data hopefully will be useful in the future to predict the properties of alloys without even running ab initio calculations or make them easier by serving values as an initial guess.

3.2.1 NiCoFeCr$_x$ alloys

I will summarize my results here comparing the lattice constants for experimental (a_{expt}) and EMTO ($a_{\text{ab initio}}$) results. The EMTO results are for 0 K, and the experimental results are extrapolated by the formulas I mentioned in the Section 2.7. The x means the mole fraction of chromium in the alloy. For $x = 1,00$, the alloy is equimolar, so every component is in the same amount – 25%– in the alloy. All the alloys are having FCC structures.

x	a_{expt}	$a_{\text{ab initio}}$	VEC
0,50	3,557	3,521	8,57
0,60	3,558	3,521	8,50
0,70	3,558	3,523	8,43
0,80	3,560	3,525	8,37
0,90	3,561	3,526	8,31
0,95	3,561	3,527	8,28
1,00	3,563	3,527	8,25
1,05	3,563	3,528	8,22
1,10	3,563	3,527	8,20
1,15	3,563	3,529	8,17

Table 8: Calculated lattice constants compared and experimental data for NiCoFeCr$_x$ alloys

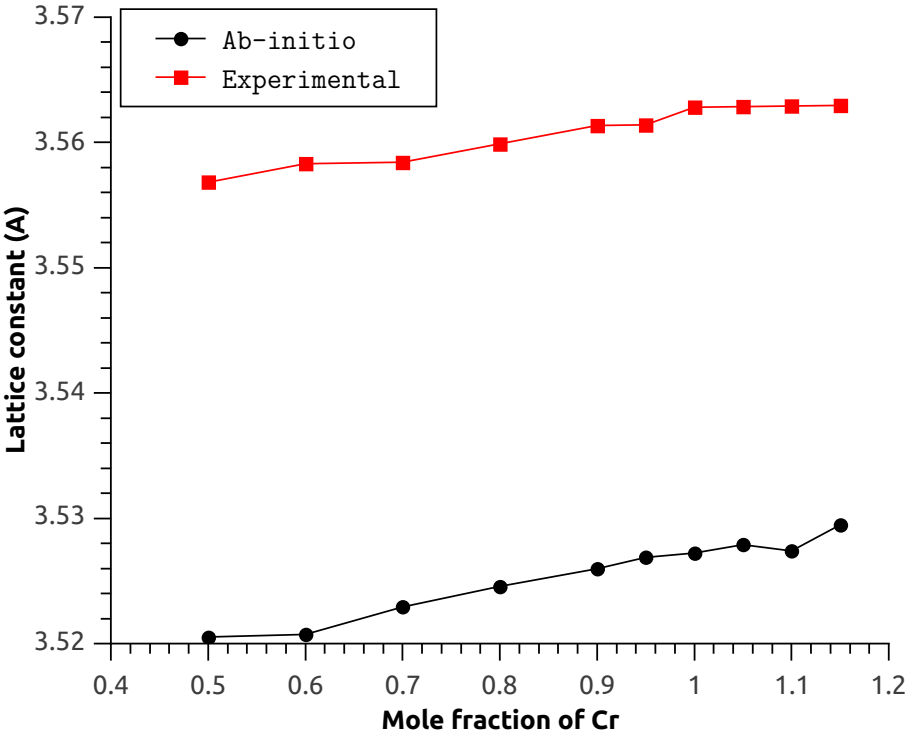

Figure 11: Comparison of lattice constants of $NiCoFeCr_x$ alloys

There is only a slight between the experimental data and the ab initio calculation. The mean absolute deviation is $0,026$ Å. The calculation is not only precise but follows the trend correctly. I believe that the zero-Kelvin approximation would be more accurate I would know the exact thermal coefficient for each alloys.

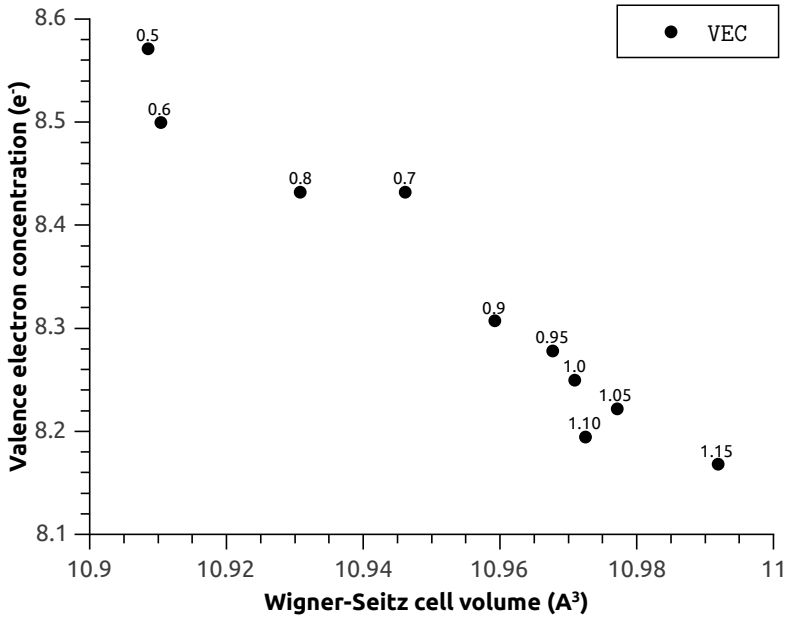

Figure 12: Valence electron concentrations of $NiCoFeCr_x$ alloys. The reader can notice that the VEC > 8, so all of the alloys are having FCC crystal structure.

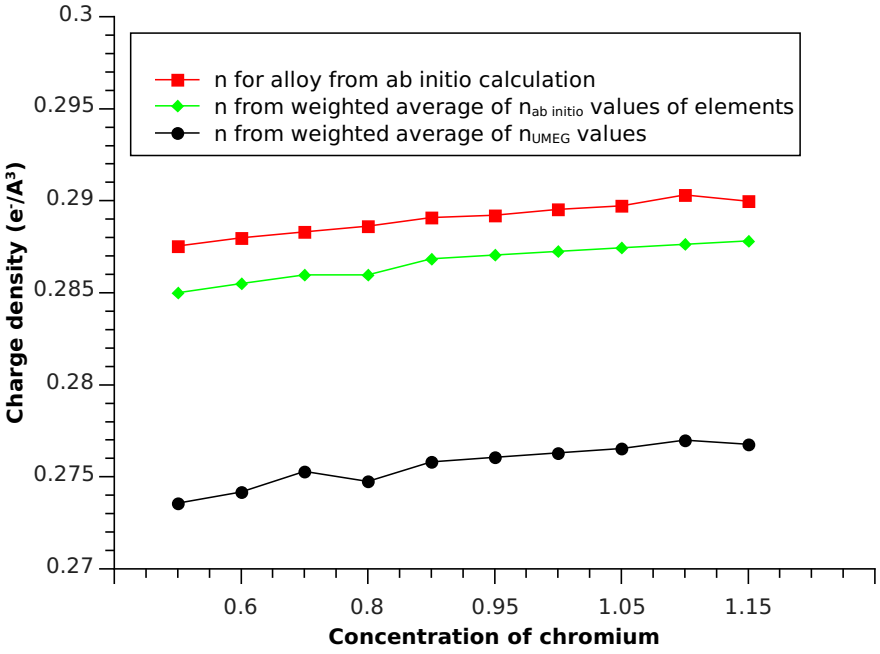

Figure 13: Valence electron densities of $NiCoFeCr_x$ alloys.

For all these three dependencies we have used Wigner-Seitz radius for calculating the electron density n. For the UMEG values the bonding valence of [26] was used.
On Figure 12 it is shown that all the VEC values are above 8 what means they have FCC structure.

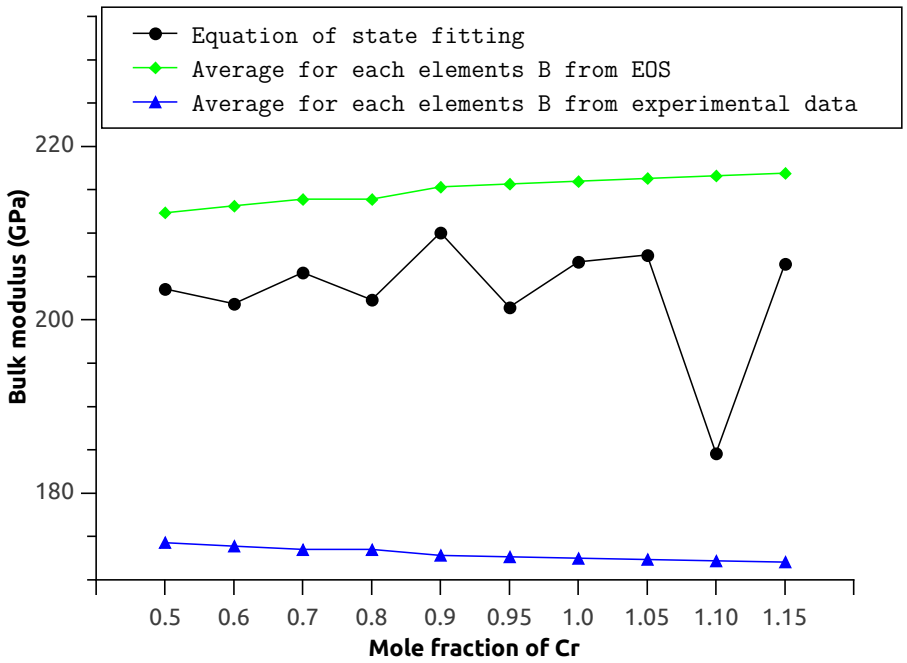

Figure 14: Different bulk moduli for NiCoFeCr$_x$ alloys

On the Figure 14 there are three different calculation methods for the bulk modulus. The black one is obtained by the fitting of the equation of state for the alloys. The green is obtained by calculating the average bulk modulus of the alloying elements from the ab inito results. The blue is obtained by calculating the average bulk modulus of the alloying elements from the experimental results. Unfortunately there are no results for real experimental measurements.

3.2.2 CuNiCoFeCrAl$_x$ alloy

I am going to present the results of experimental (a_{expt}) and EMTO ($a_{\text{ab initio}}$) datas. The x stands for the mole fraction of aluminum. The last two results are written in italic font are BCC structures, the others are FCC.

x	a_{expt}	$a_{\text{ab initio}}$	VEC
0,3	3,567	3,564	8,47
0,5	3,568	3,573	8,27
2,8	*2,885*	*2,923*	*6,73*
3,0	*2,881*	*2,936*	*6,63*

Table 9: Calculated lattice constants compared with experimental datas for CuNiCoFeCrAl$_x$ alloys

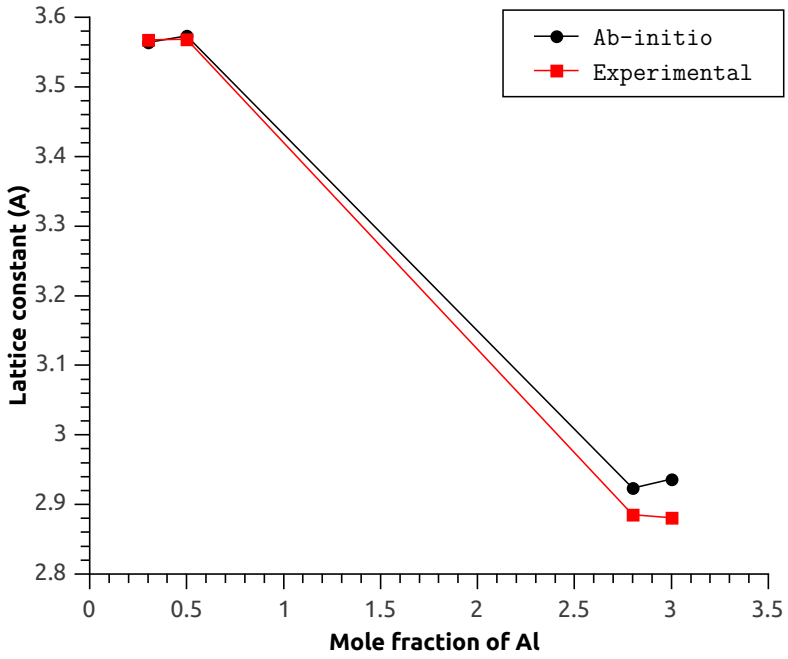

Figure 15: Comparison of lattice constants of CuNiCoFeCrAl$_x$ alloys

The ab initio performs really well for this alloy. The mean absolute deviation is $0,023$ Å. I have attached the VEC values in the Table 9 as well. The values are following the rule pretty well respectively to the crystal structure. The change of the structure can also be observed from the big jump in the values of the lattice constant.

3.2.3 NiCoFeCrAl$_x$ alloy

I am going to present the results of experimental (a_{expt}) and EMTO ($a_{\text{ab initio}}$) data. The x stands for the mole fraction of aluminum. The last two results are written in italic font are BCC structures, the others are FCC.

x	a_{expt}	$a_{\text{ab initio}}$	VEC
0,25	3,577	3,544	7,94
0,30	3,585	3,547	7,88
0,375	3,581	3,554	7,8
1,25	*2,857*	*2,863*	*7,00*
1,50	*2,869*	*2,871*	*6,81*

Table 10: Calculated lattice constants compared with experimental data for NiCoFeCrAl$_x$ alloys

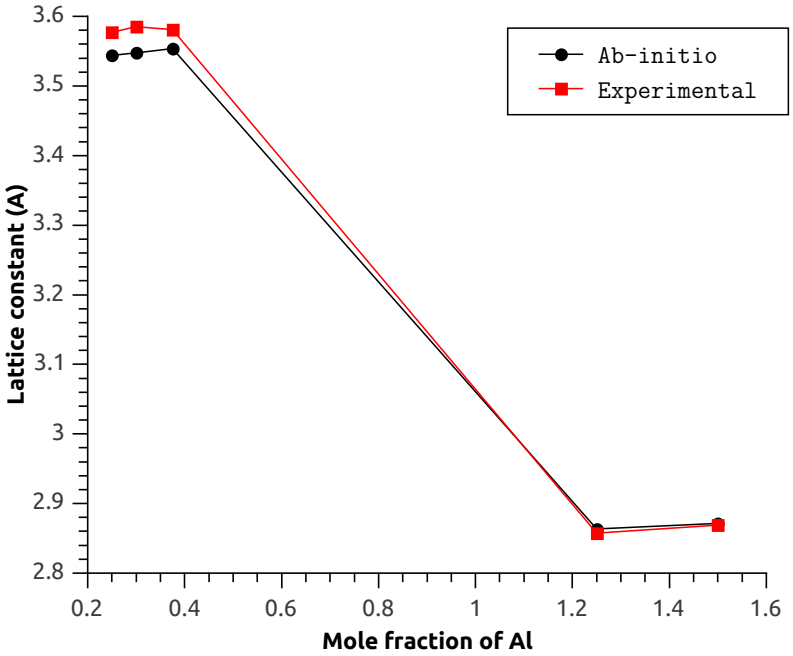

Figure 16: Comparison of lattice constants of NiCoFeCrAl$_x$ alloys

The mean absolute deviation is $0,016$ Å here. The VEC values are following the rule well respectively to the crystal structure.

3.2.4 Other alloys

At this section I am going to present the results for different kind of alloys. Most of them are containing the three principal elements such as iron, nickel and cobalt, but some of them are having other components such as refractory or noble metals. Most of them are equimolar except the $NiCoFeCrPd_2$ alloy. The alloys written in italic font are BCC alloys, the others are FCC.

#	Alloy	a_{expt}	$a_{\text{ab initio}}$
1.	NiCoFeCrMn	3,572	3,523
2.	NiCoFeCrMnNb	3,604	3,675
3.	NiCoFeCrMnV	3,564	3,574
4.	NiCoFeCrPd	3,630	3,640
5.	NiCoFeCrPd2	3,692	3,695
6.	CuNiCoFe	3,570	3,557
7.	CuNiFeCr	3,574	3,574
8.	CuNiCoFeCr	3,564	3,550
9.	*MoNbTaW*	*3,212*	*3,211*
10.	*MoNbTaVW*	*3,181*	*3,183*

Table 11: Calculated lattice constants compared with experimental data

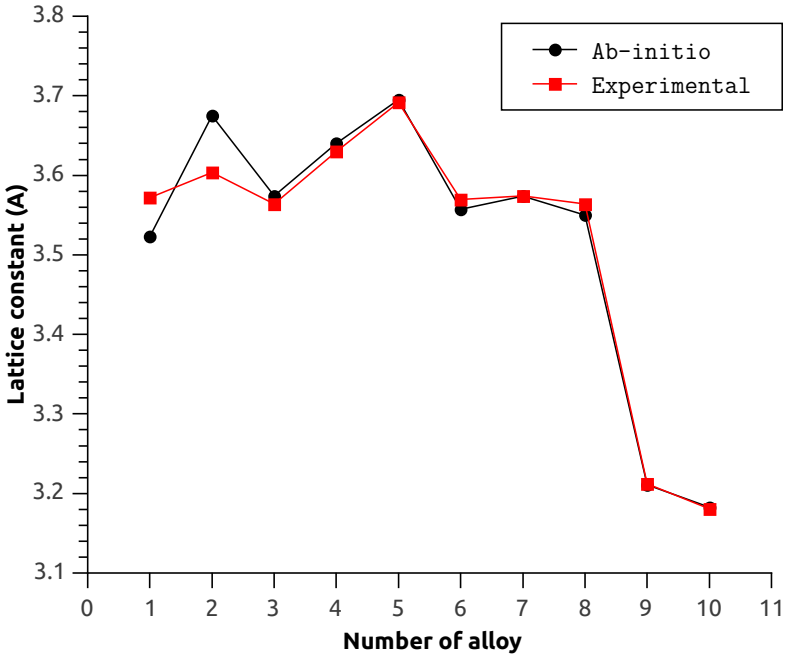

Figure 17: Comparison of lattice constants of other alloys

The results have only slight difference, the mean absolute deviation is $0,017$ Å for this group of alloys. The results for the refractory HEAs are virtually the same as the experimental ones.

3.2.5 Alloy shrinking

I would like to find out if the alloys' components are keeping their density in the alloy. My idea is to test it by calculating the density for those alloys what are having experimental data for the density. These data from Ádám Vida's measurement what he used in his thesis [31]. I collected those data and calculated different densities by different approaches.

I used the next equation to get the average density for alloys from the components' densities:

$$\overline{\rho} = \frac{\sum\limits_{i} c_i M_i}{\sum\limits_{i} c_i V_i}, \tag{77}$$

where $\overline{\rho}$ is the average density in g/cm^3, c_i is the concentration of the component, M_i is the molar mass of the element in g/mol, V_i is the atomic volume of the element in cm^3.

Three different densities have been calculated using different V_i volumes which have been calculated: V_1 as V_{WS} from ab initio, V_2 as V_{WS} from tabulated data, V_3 as V_{WS} from Goldschmidt radius. All results are at room temperature. The ρ_{expt} stands for the experimental data. These measurements were performed by Ádám Vida [31] using a helium pycnometer (AccuPyc II 1340) to obtain the densities. The samples have been obtained by casting in could mold using induction furnace.

Comparing these calculated densities with experimental data shown in Table 12 we can observe that the experimental density data are systematically above the calculated ones. This means shrinking of alloy despite the fact that it is a highly distorted structure. The explanation of this shrinking needs further investigations.

	Alloy	ρ_{expt} (g/cm^3)	ρ_1 (g/cm^3)	ρ_2 (g/cm^3)	ρ_3 (g/cm^3)
1	$Ni_{25}Fe_{50}Cr_{25}$	7,879	8,134	7,934	7,074
2	NiCoFeCr	8,343	8,350	8,182	7,364
3	CuNiCoFeCr	8,341	8,421	8,336	7,654
4	$V_{90}Fe_{10}$	6,327	6,436	6,247	5,863
5	$V_{80}Fe_{20}$	6,568	6,591	6,405	6,022
6	$V_{70}Fe_{30}$	6,777	6,751	6,569	6,187
7	$Ni_xCo_xFe_xCr_xAl_{6.976}$ $x = 23.255$	7,811	7,135	7,036	6,471
8	$Ni_xCo_xFe_xCr_xAl_{11.11}$ $x = 22.22$	7,188	7,452	7,341	6,712
9	$Ni_xCo_xFe_xCr_xAl_{24.528}$ $x = 18.867$	6,861	6,426	6,427	5,980
10	$Ni_xCo_xFe_xCr_xAl_{27.272}$ $x = 18.181$	6,688	6,243	6,252	5,837
11	$Ni_xCo_xFe_xCr_xAl_{33.356}$ $x = 16.661$	6,400	6,061	6,082	5,697
12	NiCoFeCrAl	7,013	6,737	6,724	6,221
13	$Ni_{38.33}Fe_{36}Cr_{13.88}Mo_{6.66}W_{5.15}$	9,650	9,249	9,126	8,487
14	$Ni_{29.5}Fe_{39.8}Cr_{20}Mo_6W_{4.7}$	9,159	9,056	8,905	8,088
15	$Ni_{35}Fe_{30}Cr_{20}Mo_{10}W_5$	8,995	9,239	9,115	8,296
16	NiFeCrMoW	11,195	11,260	11,214	10,158
Mean absolute deviation			0,234 (2,994%)	0,250 (3,189%)	0,818 (10,451%)

Table 12: Comparison for different calculation methods for densities of alloys with experimental data. ρ_1 from Eq. (77) with V_{WS} from ab initio, ρ_2 from Eq. (77) with V_{WS} from tabulated data, ρ_3 from Eq. (77) with V_{WS} from Goldschmidt radius.

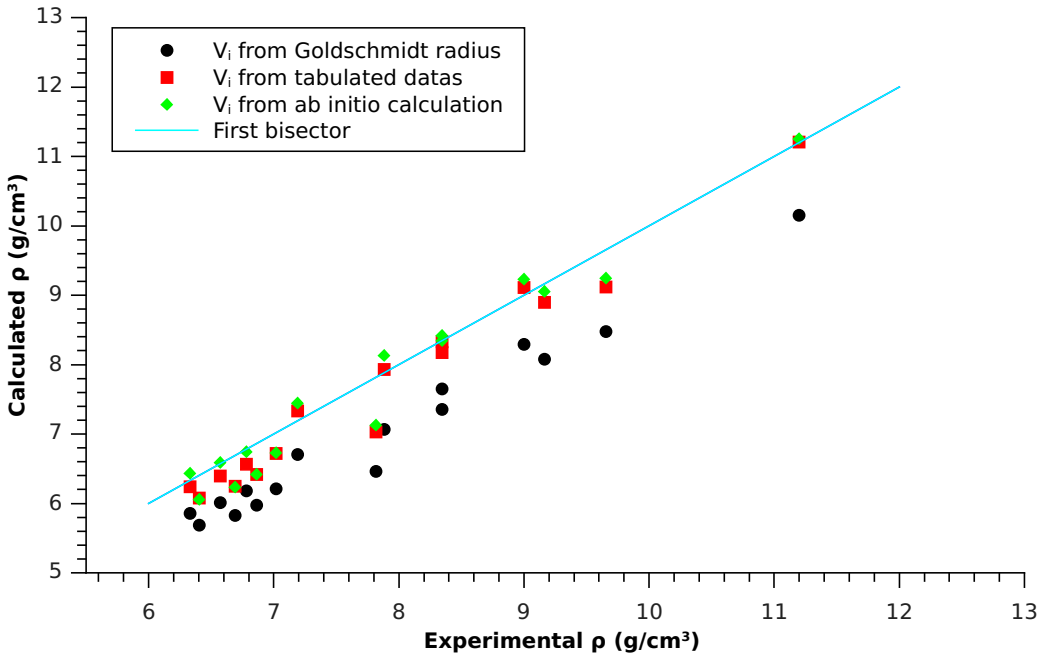

Figure 18: Comparison of densities calculated by using different V_i values for (77)

Figure 18 shows that the data from ab initio and tabulated data scatters around the first bisector whereas those calculated with Goldschmidt atomic radius are systematically below of it.

The mean absolute deviation of the data from the experimental data have been calculated for the three different densities by the next formula:

$$\mathrm{MAD} = \frac{1}{n}\sum_{i=1}^{i} |f_i - y_i|, \tag{78}$$

where n is the number of the values, f_i is the ith experimental data and y_i is the ith calculated value for density: ρ_1, ρ_2 or ρ_3, respectively.

4 Discussion

Element	$a_{\text{ab initio}}$ (Å)	a_{expt} (Å)		B_{expt} (GPa)	$B_{\text{ab initio}}$ (GPa)
Al	4,019	4,020		76	81,36
V	3,023	3,024		160	166,33
Cr	2,800	2,877		160	241,56
Mn	2,925	2,910		120	247,15
Fe	2,850	2,853		170	162,05
Co	2,485	2,498		180	256,75
Ni	3,508	3,508		180	203,61
Cu	3,602	3,595		140	161,76
Nb	3,288	3,294		170	155,90
Mo	3,136	3,141		230	229,10
Pd	3,883	3,875		180	197,07
Ta	3,282	3,299		200	189,01
W	3,168	3,160		310	310,42
Deviations					
Mean absolute deviation		0,093		-	30,30

Table 13: Summary of calculated elements

In Table 13 the experimental and calculated B values are also shown. In this case the agreement is not always acceptable especially for Mn, Cr and Co we have found more than 50% deviations from the experimental data. Similarly deviations for the pure elements have been reported by[10], see Table 7.1 at page 129.

x	a_{expt} (Å)	$a_{\text{ab initio}}$ (Å)	VEC
$NiCoFeCr_x$			
0,50	3,557	3,521	8,57
0,60	3,558	3,521	8,50
0,70	3,558	3,523	8,43
0,80	3,560	3,525	8,37
0,90	3,561	3,526	8,31
0,95	3,561	3,527	8,28
1,00	3,563	3,527	8,25
1,05	3,563	3,528	8,22
1,10	3,563	3,527	8,20
1,15	3,563	3,529	8,17
$CuNiCoFeCrAl_x$			
0,3	3,567	3,564	8,47
0,5	3,568	3,573	8,27
2,8	*2,885*	*2,923*	*6,73*
3,0	*2,881*	*2,936*	*6,63*
$NiCoFeCrAl_x$			
0,25	3,577	3,544	7,94
0,30	3,585	3,547	7,88
0,375	3,581	3,554	7,8
1,25	*2,857*	*2,863*	*7,00*
1,50	*2,869*	*2,871*	*6,81*
Other			
NiCoFeCrMn	3,572	3,523	8,00
NiCoFeCrMnNb	3,604	3,675	7,50
NiCoFeCrMnV	3,564	3,574	7,50
NiCoFeCrPd	3,630	3,640	8,60
NiCoFeCrPd2	3,692	3,695	8,83
CuNiCoFe	3,570	3,557	9,50
CuNiFeCr	3,574	3,574	8,75
CuNiCoFeCr	3,564	3,550	8,80
MoNbTaW	*3,212*	*3,211*	*12,50*
MoNbTaVW	*3,181*	*3,183*	*11,00*
Deviations			
Mean absolute deviation		0,019	-

Table 14: Summary of calculated alloys

In Table 14 are shown the lattice constants are for the alloys considered in this thesis, both experimental obtained by XRD and by ab initio calculations using QNA exchange correlation approximation. The deviation of the calculated values are less than $0,019$ Å which is a rather good estimation of the experimental data. The ab initio calculation have been repeated used PBE (GGA) approximation as well and we have got a slightly larger deviation from the experimental data, $0,022$Å. This shows the strength of the ab initio calculations for HEAs.

In the case of alloys we have found again good agreement between the experimental and ab initio calculations for the lattice constant, see Table 14. The bulk modulus, B values calculated only for a few single phase HEAs and compared with the experimental data of Vida [31].

Alloy	$B_{\text{ab initio}}$	B_{expt}
NiCoFeCr	206,7	128,5
$NiCoFeCrAl_{0.3}$	190,9	146,3
NiCoFeCrAl	192,43	173,9
$NiCoFeCrAl_{1.5}$	156,22	160,8

Table 15: Comparison between ab initio calculated and measured bulk modulis

For the bulk modulus B however the calculation values for single phase HEAs shows large deviations from the experimental one [31]. The explanation for these deviations needs further investigations.

5 Summary

- The EMTO Program Package of professor Levente Vitos is a powerful ab initio calculation tool to get reasonable results concerning the physical and mechanical properties of the alloys.
- The QNA version of the program is more accurate than the PBE one.
- We have found good agreement between the calculated and experimental lattice values.
- We have found good agreement between the ab initio electron density values compared to those calculated from bonding valence and tabulated volume per atom data.
- We have found poor agreement concerning the calculated and experimental bulk modulus values both for elements and alloys.
- We have found good agreement between the calculated and measured densities for single-phase HEAs.
- The measured densities for two-phase HEAs are systematically above the calculated one which can be interpreted as a shrinkage of the structure compared to the ideal hard sphere structure.

6 What next

We intend to form an ab initio database (lattice constant, Young's-, bulk-, and shear modulus) for all the BCC and FCC single-phase HEAs published so far. It is challenging to improve the EOS method for calculation of bulk modulus in order to get a better agreement with the experimental data. A better B/G ratio would help to predict more accurate the brittleness of HEAs. These tasks will be solved during the forthcoming PhD thesis.

References

[1] B.S. Murty, Jien-Wei Yeh and S. Ranganathan, High Entropy Alloys (Elsevier Inc. 2014)

[2] Jien-Wei Yeh, Swe-Kai Chen, Su-Jien Lin, Jon-Yiew Gan, Tsung-Shune Chin, Tao-Tsung Shun, Chun-Huei Tsau, and Shou-Yi Chang, ADVANCED ENGINEERING MATERIALS 6, No. 5 (2004)

[3] Fuyang Tian, Lajos Karoly Varga, Nanxian Chen, Lorand Delczeg, and Levente Vitos PHYSICAL REVIEW B87, 075144 (2013)

[4] Fuyang Tian, Ab initio atomistic simulation of metals and multicomponent alloys, PhD thesis (KTH - Stockholm, 2013)

[5] Fuyang Tian, Lorand Delczeg, Nanxian Chen, Lajos Varga, Jiang Shen, and Levente Vitos, Physical Review B88, 085128 (2013).

[6] P. Hohenberg and W. Kohn, Phys. Rev.136, B864 (1964).

[7] W. Kohn and L. J. Sham, Phys. Rev.136, A1133 (1965).

[8] L. Vitos, H. L. Skriver, B. Johansson and J. Kollár, Comp. Mat. Sci. 18, 24 (2000).

[9] L. Vitos, Phys. Rev. B 64, 014107 (2001).

[10] L. Vitos, Computational Quantum Mechanics for Materials Engineers: The EMTO Method and Applications, Engineering Materials and Processes Series (Springer-Verlag, London, 2007).

[11] Soven, P.: Phys. Rev. 156, 809 (1967)

[12] Taylor, D. W.: Phys. Rev. 156, 1017 (1967)

[13] Györffy, B. L.: Phys. Rev. B 5, 2382 (1972)

[14] J. P. Perdew, K. Burke, and M. Ernzerhof, Phys. Rev. Lett. 77, 3865 (1996).

[15] H. Levämäki, M. P. J. Punkkinen, and K. Kokko, L. Vitos, PHYSICAL REVIEW B 86, 201104(R) (2012)

[16] H. Levämäki, M. P. J. Punkkinen, and K. Kokko, L. Vitos, PHYSICAL REVIEW B 89, 115107 (2014)

[17] Neil W. Ashcroft, N. David Mermin, Solid State Physics, 1st edition, Brooks Cole (1976)

[18] W. M. Haynes, CRC Handbook of Chemistry and Physics, 94th Edition, CRC Press (2013)

[19] L. H. Nosanow, Journal of Low Temperature Physics, Vol. 26, Nos. 3/4, 1977

[20] Philipp Haas, Fabien Tran, and Peter Blaha, PHYSICAL REVIEW B 79, 085104 (2009)

[21] Gábor I. Csonka, John P. Perdew, Adrienn Ruzsinszky, Pier H. T. Philipsen, Sébastien Lebègue, Joachim Paier, Oleg A. Vydrov, and János G. Ángyán, PHYSICAL REVIEW B 79, 155107 (2009)

[22] Sheng Guo, Chun Ng, Jian Lu, and C. T. Liu, J. Appl. Phys. 109, 103505 (2011)

[23] Jien-Wei Jeh, JOM, Vol. 65, No. 12, 2013

[24] Fuyang Tian, Lajos K. Varga, Nanxian Chen, Jiang Shenb, Levente Vitos, Intermetallics Volume 58, March 2015, Pages 1–6

[25] Kazimierz F. Wojciechowski, Physica B, 229, 55-62 (1996)

[26] H,B. Shore and J.H. Rose, Phys. Rev. Lett. 67 3045 (1991).

[27] H. Bakker, Enthalpies in Alloys: Miedema's Semi-Empirical Model, Trans Tech Publications, Zurich, 1998.

[28] A.M. James and M.P. Lord in Macmillan's Chemical and Physical Data, Macmillan, London, UK, 1992.

[29] G.W.C. Kaye and T.H. Laby in Tables of physical and chemical constants, Longman, London, UK, 15th edition, 1993.

[30] G.V. Samsonov (Ed.) in Handbook of the physicochemical properties of the elements, IFI-Plenum, New York, USA, 1968.

[31] Ádám Vida, Preparation and investigation of high entropy alloys, Master's thesis, Eötvös Loránd Universty - Budapest (2015)

NYILATKOZAT

Név: Molnár Dávid Sándor

ELTE Természettudományi Kar, szak: Anyagtudomány MSc

ETR azonosító: ENT9FB

Diplomamunka címe:
Investigation of the properties of high entropy alloys by ab initio calculations

A **diplomamunka** szerzőjeként fegyelmi felelősségem tudatában kijelentem, hogy a dolgozatom önálló munkám eredménye, saját szellemi termékem, abban a hivatkozások és idézések standard szabályait következetesen alkalmaztam, mások által írt részeket a megfelelő idézés nélkül nem használtam fel.

Budapest, 2015.05.29.

_____

a hallgató aláírása